A Review: Neural-Inspired Photonic Functional Systems for Dynamic RF Signal Processing

Mable P. Fok

(Invited Paper)

***Abstract*—Drawing inspiration from our nature, photonic systems that use light to imitate neural algorithms and behaviors of nature could be effective to solve complex problems in human's civilized society that have been challenging for conventional electronic to tackle. Since neural algorithms are natural designs that have undergone hundreds of million years of evolution and govern the survival of the organism, therefore, those neural algorithms are highly effective for the designated tasks. The goal of this article is to review the recent demonstrations of the photonic implementations of small scale functional neural algorithms for dynamic RF signal processing applications. In this article, two small-scale neural algorithms are reviewed – (i) spike timing dependent plasticity, an algorithm that governs how neural network are connecting together and how learning/adaptation can be achieved in animals, and (ii) jamming avoidance response in Eigenmannia, an algorithm in a gene of electric fish that mitigates frequency jamming between neighboring electric fish. The photonic circuits that are inspired by the two neural algorithms are also presented and the real-life applications of the neural algorithms in human society will be discussed.**

***Index Terms*—Neural-inspired photonics, biomimetic photonics, photonic neuron, bio-inspired signal processing, neural algorithm.**

I. Introduction

LIVING organisms have undergone hundreds of million years of evolution and have been well adapted to their environment. Adaptation governs how living organisms look, how they behave, how they are built, and how they live their life, such that the living organisms can suit to survive and reproduce in their habitats. The neural algorithms that govern how living organisms behave are critical for their survival and are extremely efficient in performing their designed tasks. Due to the civilization of human society, powerful technologies are invented but that also bring unsolved challenges that are beyond what our current technologies could offer. Looking back to our uncivilized nature, there are lots of adaptation schemes and neural algorithms that could be the natural solutions towards the critical challenges that we are facing in modern technologies. It is exciting to discover, reveal, and understand those powerful neural algorithms, as well as mimicking them using photonics to make them as effective solutions for the challenges we are facing in human society.

In the last ten years, intensive research efforts have been made in various areas related to marrying photonics with neural science. For example, spike processing devices [1]–[18] using semiconductor optical devices, silicon photonics, and excitable lasers have been proposed and experimentally demonstrated to mimic the behavior of a leaky integrate and fire neuron. The photonic based spiking devices could operate at a tens of picosecond time scale while mimic the spiking process in a biological neuron, including summing and weighting, integration, thresholding, and spiking. Synapse in neural network that governs the processing and storage of information in the brain has been mimic using photonics [19]–[22] that could potentially allow photonic neural network to process information like the brain. Photonic neural networks have also been proposed using VCSELs-SA [23] and nanophotonic chip with wavelength division multiplexing techniques [24]. Small scale photonic systems inspired by functional neural algorithms have been demonstrated using semiconductors and silicon photonics for performing specific tasks [25]–[28] including pattern recognition, supervised learning, and jamming avoidance. Furthermore, a number of neural algorithms inspired photonic circuits have been demonstrated with success and shown their potentials in solving challenges in dynamic RF systems. For example, a photonic circuit that consists of two semiconductor optical amplifiers (SOA) as the neuron has been used to experimentally demonstrate the tail-flip escape response in crayfish [29]. The tail-flip escape response is a fast and accurate algorithm that allows the crayfish to escape from danger quickly, while it has been successfully used for pattern recognition in the corresponding photonic escape response circuit. Furthermore, spike timing dependent plasticity (STDP) - a biological algorithm that governs various types of learning in human and animals by adjusting the interconnection strength between neurons has been mimicked using a SOA [30], VCSOA [32], high-order passive ring resonators, as well as a SOA with an electro-absorption modulators [34]. A photonic circuit that performs supervised learning based on STDP has been demonstrated experimentally [34], [35] where the neuron learnt how the teacher teaches it during the learning phase. More recently, machine learning based on photonics neural circuits [36]–[40] has drawn intensive research interest.

Manuscript received February 14, 2020; revised April 14, 2020; accepted May 5, 2020. Date of publication May 11, 2020; date of current version October 1, 2020. This work is supported by National Science Foundation under Grants ECCS 1342177, CMMI 1400100, and ECCS 1653525.

The author is with the Lightwave and Microwave Photonic Laboratory, College of Engineering, University of Georgia, Athens, GA 30602 USA (e-mail: mfok@uga.edu).

Color versions of one or more of the figures in this article are available online at https://ieeexplore.ieee.org.

Digital Object Identifier 10.1109/JLT.2020.2993292

This paper focuses on the review of recent progress on mimicking small-scale functional neural algorithms with photonics and its applications in solving challenges in human technologies. First, the biological spike timing dependent plasticity (STDP) algorithm that governs learning will be introduced, and its applications and implementation in angle-of-arrival detection and 3D localization [30], [31] will be explained and discussed. Next, the jamming avoidance response of Eigenmannia - a genus of electric fish [41]–[44] will be dissected, and the use of photonic phenomena to mimic the jamming avoidance response will be discussed [44]. Finally, the investigation of using the photonic jamming avoidance circuit for mitigating inadvertent jamming in RF system and phase locking will be presented [45].

II. Spike Timing Dependent Plasticity (STDP)

The most fascinating feature of neuron is its ability to learn and adapt, which governs how we should act, allows us to think, alters the state of our internal organ, and enables us to have memory. Neuron networks achieve the amazing ability to learn, think, and remember greatly relying on the synaptic weight plasticity between neurons. Synaptic weight plasticity enables neural systems to adjust the strength of synaptic connection between neurons based on the information being processed and the response of the neuron itself. While there are a number of synaptic weight plasticity models, spike timing dependent plasticity (STDP) is the most popular one. STDP has a number of variations (e.g. additive type STDP, quadratic type STDP, reverse STDP) but generally it is a biological process that adjust the interconnection strength between neurons based on the temporal relationship between pre-synaptic and post-synaptic activities. An old saying in neural science community describes STDP as "Neurons that fire together wire together". That means the more you are running certain neural circuit, the stronger the circuit become. To enable learning, adaptation, and memory in photonic neural circuit, the ability to mimic STDP using photonics is essential. In fact, photonic based STDP circuits have been demonstrated [34], [35] and have shown that the photonic based STDP behavior could be operated at a hundred of picosecond time scale. Furthermore, supervised learning based on photonic based STDP has been demonstrated [34], [35] to get a taste of the possibility to build a fast learning neural network using photonic technologies.

A. Biological STDP and Optical STDP

Here, we are discussing the most common STDP [46] that causes long-term potentiation (LTP) and long-term depression (LTD) of synaptic connections. The interconnection strength between two biological neurons is governed by STDP, which is determined by the relative timing and sequence between the pre-synaptic and post-synaptic spikes, as illustrated in Fig. 1(a). Pre-synaptic spike (red) is the output spike from neuron 1 (N1) that also acts as the stimulating input of neuron 2 (N2), while post-synaptic spike (blue) is the output spike from neuron 2 (N2). If N2 spikes shortly after the receiving of stimulation from the pre-synaptic spike (i.e. pre-synaptic spike is leading the post-synaptic spike), the interconnection strength will be significantly increased, resulting in potentiation of the connection strength, as illustrated by the shaded purple region in Fig. 1(b). On the other hand, if N2 spikes before receiving the stimulation from the pre-synaptic spike (i.e. pre-synaptic spike is lagging from the post-synaptic spike), the interconnection strength will be significantly decreased, resulting in depression of the connection strength, as illustrated by the shaded brown region in Fig. 1(b). The exact amount of synaptic connection strength increment/decrement depending on the precise timing difference between the pre-synaptic and post-synaptic spikes of the neuron. A smaller time difference will result in a larger change in synaptic connection strength, while a larger time difference will result in a smaller change in synaptic connection strength, as shown in Fig. 1(b).

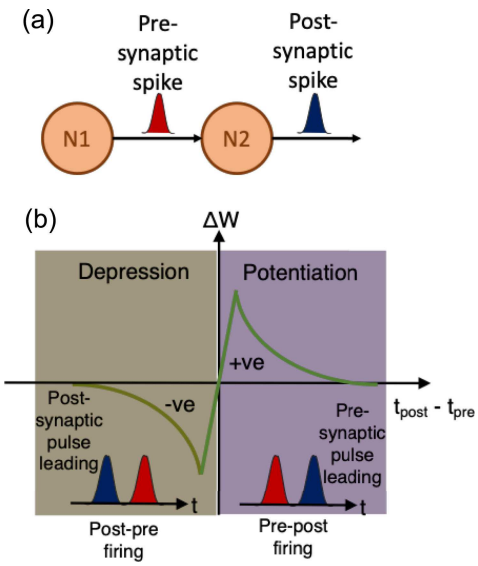

Fig. 1. (a) Illustration of pre-synaptic and post-synaptic spikes from two neurons. (b) Illustration of a spike timing dependent plasticity curve. Pre-post firing (right purple region): post synaptic spike fires shortly after the pre-synaptic spike; Postpre-firing (left brown region): post synaptic spike fires before the pre-synaptic spike. t_{post}-t_{pre}: time difference between the firing of the post- and pre-synaptic spikes.

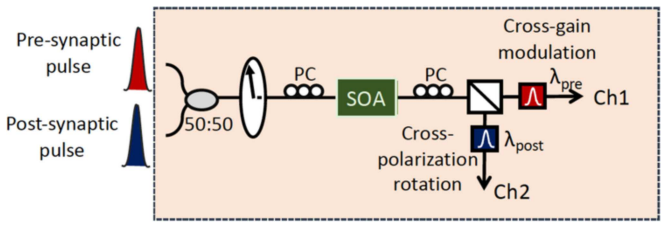

Fig. 2. Schematic diagram of the photonic based STDP. PC: polarization controllers; SOA: semiconductor optical amplifier.

In biological neuron, the STDP control is an internal backward feedback that changes the weight of the synaptic connection. While in photonic based neurons, the control of weight change can be performed either through an internal response or external feedback. STDP with internal weight response is suitable for implementing large scale photonic neural network, while standalone photonic STDP circuit has the advantage of being used in RF signal processing without a large-scale neural network. To mimic STDP using photonics, a single semiconductor optical amplifier (SOA) is used, as illustrated in Fig. 2. First, both the pre- and post-synaptic pulses are combined using an optical coupler and launched to the SOA via a polarizer to ensure

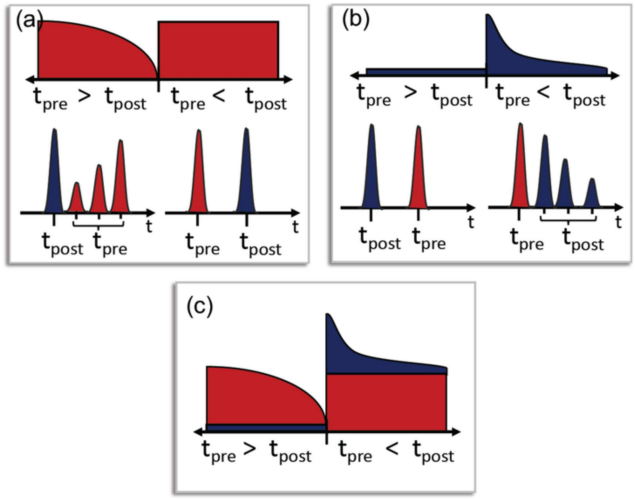

Fig. 3. (a) Illustration of the dependency of cross-gain modulation effect on the pulse timing and sequence. (b) Illustration of the dependency of crosspolarization rotation effect on the pulse timing and sequence. (c) Resultant STDP response based on photonic phenomena.

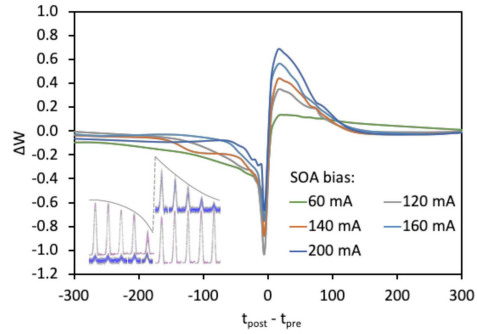

Fig. 4. Experimentally measured STDP curves from the photonic based STDP circuit. Inset: Individually measured output pulses at channel 1 and channel 2.

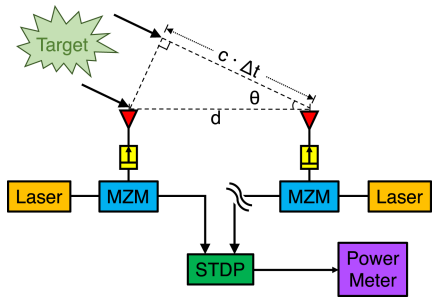

Fig. 5. Experimental setup of STDP based AOA measurement. MZM: electrooptic intensity modulator; STDP: photonic based spike-timing dependent plasticity circuit.

the optimized polarization state of light is used. Inside the SOA, there are two optical phenomena occurring – cross-gain modulation and cross-polarization rotation. At the output of the SOA, a polarization beam splitter is used to observe the power change at the pre-synaptic pulse (channel 1) and post-synaptic pulse (channel 2).

For channel 1, the post-synaptic pulse is the pump light that induces cross-gain modulation effect, while the pre-synaptic pulse is the probe signal that experiences the effect. Cross-gain modulation effect contributes to the power change in pre-synaptic pulse according to the timing and sequence, as illustrated in Fig. 3(a). If the post-synaptic pulse is leading the pre-synaptic pulse (post-pre firing), then the post-synaptic pulse depletes the carriers in the SOA and the pre-synaptic pulse will experience insignificant gain at the SOA that results in a weak output power. Cross-gain modulation effect is weaker if the probe signal enters the SOA much later than the pump signal. On the other hand, if the pre-synaptic pulse is leading the post-synaptic pulse (pre-post firing), then the post-synaptic pulse is not able to induce cross-gain modulation to the pre-synaptic pulse, pre-synaptic pulse will experience large gain and resulting in a strong output power at the output pre-synaptic pulse. For channel 2, the pre-synaptic pulse is the pump light that induces cross-polarization rotation, while the post-synaptic pulse is the probe signal that experiences the effect. Cross-polarization rotation effect contributes to the power change in post-synaptic pulse according to the timing and sequence, as illustrated in Fig. 3(b). Initially, the polarization of the input post-synaptic pulse is set such that no power is observed after the polarization beam splitter for channel 2. If the pre-synaptic pulse is leading, it will introduce cross-polarization rotation to the post-synaptic pulse, such that significant power can be observed at channel 2. Cross-polarization rotation is weaker if the probe signal goes into the SOA at a much later time. On the other hand, when the post-synaptic pulse enters the SOA before the pre-synaptic pulse, no cross-polarization rotation can be induced, and no output power is observed in channel 2. By combining the power from both channel 1 and channel 2, a STDP response is observed as shown in Fig. 3(c).

The experimentally measured channel 1 and channel 2 outputs are shown in the inset in Fig. 4, and the corresponding measured STDP response based on the use of SOA and photonic phenomena is shown in Fig. 4. It is worth noticing that once the polarization setting is determined, there is no need to further adjust the polarization during the STDP measurement.

B. STDP Algorithm For Angle-of-Arrival Detection and 3D Localization

Needless to say, photonic STDP will have significant application in learning and adaptation in photonic neural systems, it is also interesting to identify the application of STDP response in engineering applications for advancing different aspects in various fields. One example is the utilization of STDP in angle-of-arrival (AOA) detection and 3D localization. Fig. 5 shows an AOA system that is based on the photonic STDP circuit [31]. Since the STDP response is strongly depending on the timing and sequence of the pre- and post-synaptic pulses, it aligns very well with the scenario of AOA detection where the actual target angle is governed by the pulses received by the two co-located antennae. The STDP based AOA system consists of two laser sources at λ_{pre} and λ_{post}, two electrical impulse generators, two Mach-Zehnder intensity modulators (MZMs), two microwave antennae, and a photonic STDP system as described in Fig. 2 [30], [31]. A microwave signal is emitted from the target object

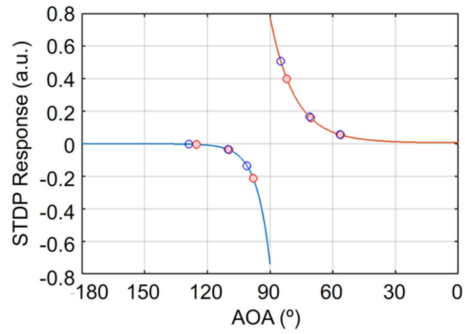

Fig. 6. Angle-of-arrival measurement based on STDP curve. Comparison of expected (red) and observed (blue) STDP outputs for various arrival angles.

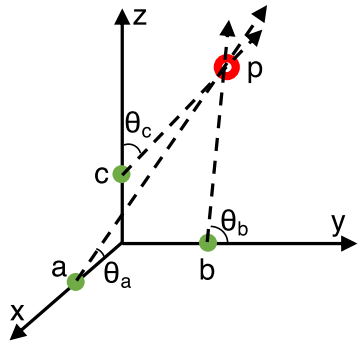

Fig. 7. Basic 3D AOA localization schematic with three nodes uncovering three directions, θa, θb, θc.

at a frequency f_{RF}, and is received by the two antennas at the AOA system.

Due to the path difference between the target and the two antennas, a time delay Δt between the two received signals is resulted. Furthermore, since the unique STDP curve is capable of distinguishing the order of the two incoming pulses (through the negative and positive values of Δt), therefore, the STDP system not just able to detect the arrival angle that is in the form of a cone shape, but it also able to identify the direction of the incoming signal that essentially pin-point the exact direction and angle of the target. The ability to distinguish negative and positive values of Δt eliminates the confusion of signals arriving from opposite directions but at the same angle relative to the antenna array. The measured STDP output value has a direct correspondent to a particular delay, which in turns is used for determining the angle-of-arrival through the relationship $c \cdot \Delta t = d \cdot \cos\theta$, where c is the speed of light, Δt is the time delay between the two received signals, d is the separation of the two antennas, and θ is the resultant angle-of-arrival value. The major advantages of STDP based AOA system are the ability to distinguish the arrival direction with the same angle, as well as having a wide detection angle that is not limited by the optical filter bandwidth as in sideband modulation-based AOA approaches. However, the compatibility of STDP based AOA with existing geolocation systems have yet to be evaluated.

Figure 6 shows the simulation results of the angle-of-arrival system. The red and blue curves correspond to the expected STDP response when the target is between 0° to 90° and 90° to 180°, respectively. When the target object is placed at an arbitrary location and emit an RF signal, the photonic STDP circuit will be able to identify its angle and direction using the STDP output value. Experimental results are shown by the hollow circles in Fig. 6, where blue circles corresponding to the observed STDP outputs for different nodes, while red hollow circles corresponding to the expected STDP output without errors. The demonstrated STDP AOA system is designed for indoor use, therefore, unit displacement with 1-mm error and laser power error of 0.003 dBm are considered in the simulation, which results in AOA measurement error $<0.5°$.

With the success of angle-of-arrival detection using STDP based circuit, 3D localization system can be implemented with three or more STDP based angle-of-arrival systems, as depicted

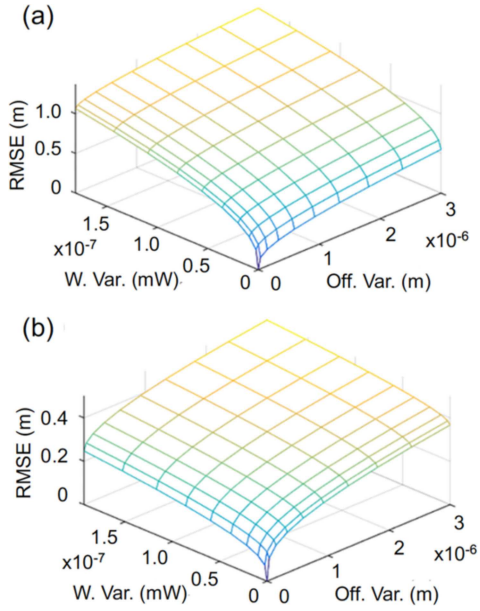

Fig. 8. Error plot for detecting a transmitter at (10, 10, 10) (a) with nodes at $x_a = y_b = z_c = 1$ m; (b) with nodes at $x_a = 1$ m, $y_b = z_c = 5$ m.

in Fig. 7. The target or transmitter is at position *p*, while the localization system consists of three STDP-based AOA nodes, each positioned on a Cartesian axis at (x_a, 0, 0), (0, y_b, 0), and (0, 0, z_c) at points a, b, and c, respectively. Each node has a transmitter/receiver that provides one third of the location information of the user at *p*. Each node acts as an angle-of-arrival unit, and the resultant value at each node forms a conical surface for each axis. The exact location of the user can be determined through the common intersection of the three conical surfaces.

To investigate the accuracy of the STDP based 3D localization system, root mean square error (RMSE) of the localization system is simulated for various scenarios. In the simulation, maximum location error is 1 mm and laser instability are 0.003 dBm for each node. Two examples of the scenarios are shown in Fig. 8. First, the transmitter is located at $x_a = y_b = z_c = 1$ m, and a maximum RMSE is just over 1 m. When the transmitter at two of the nodes are moved to $y_b = z_c = 5$ m, the RMSE is significantly reduced to 0.4 m. The maximum RMSE is further decreased to 0.3 m if the nodes are relocated to $x_a = y_b = z_c = 15$ m.

The simulation results show that the 3-node STDP based 3D localization system could provide a simple but accurate solution to indoor positioning systems, where existing systems usually require a much larger networks of measuring units [15]–[17].

The above results show the ability to perform indoor 3D localization, however, the 3-node STDP system is also capable and effective of performing outdoor positioning. The system has been explored by setting the nodes at $x_a = y_b = z_c = 5$ m and user location could be over 100 m away. A RMSE of about 9.7 m is resulted for outdoor positioning, showing that the system is also promising in outdoor positioning.

III. Jamming Avoidance Response in Eigenmannia

With neural circuits that has more than two neurons, the neural circuit could perform more complicated task. The neural algorithm that governs the mitigation of signal jamming in electric fish has been studied and has shown promising results toward tackling the same types of signal jamming in our communication systems. Eigenmannia [47]–[51], a genus of electric fish that lives under the deep ocean, generates and uses electric fields for specialized active sensing that enables navigation, communication, and prey capture in the dark. However, there is no centralized system to assign a particular frequency for a particular fish, thus, when two nearby Eigenmannia are emitting electric fields that are very similar in frequency, jamming could occur and endanger the Eigenmannia. If the electric field is being jammed by another Eigenmannia, the electric fish will lose its ability to sense its surrounding and will be unable to escape from dangers. In fact, Eigenmannia has a very efficient neural algorithm, named Jamming Avoidance Response (JAR), that always regulate the frequency of the Eigenmannia away from the other electric fish if a similar frequency is detected, and they will never cross their frequency which could increase the effect of interference.

A. Principle of The Biological JAR Model

JAR in Eigenmannia has been studied by neuroscientists and the JAR algorithm for the electric fish to mitigate jamming has been dissected. The ability for the Eigenmannia to avoid jamming from another close-by electric fish is based on the phasor phenomenon [47]–[51], where phase and amplitude information between the Eigenmannia's own electric field and the interacting electric field with the neighboring fish are used to determine how the Eigenmannia should response to any potential jamming.

The JAR in Eigenmannia can be explained using the illustration in Fig. 9. In JAR, the first Eigenmannia receives its own signal (reference signal, J_R, blue dash curve) alongside with the jamming signal f_J, that results in a beat signal at f_B (magenta solid curve) that has an envelope with frequency equals to the difference between f_J and f_R. The envelope of the beat signal is represented by the green solid curve in Fig. 9. While the waveforms in both $f_R > f_J$ and $f_R < f_J$ looks similar, a unique amplitude and phase relationship between f_R and f_B is observed. As shown in Fig. 9(a), where the jamming signal f_J is at a lower frequency than the Eigenmannia's own signal f_R, phase relationship between the beat signal and the reference

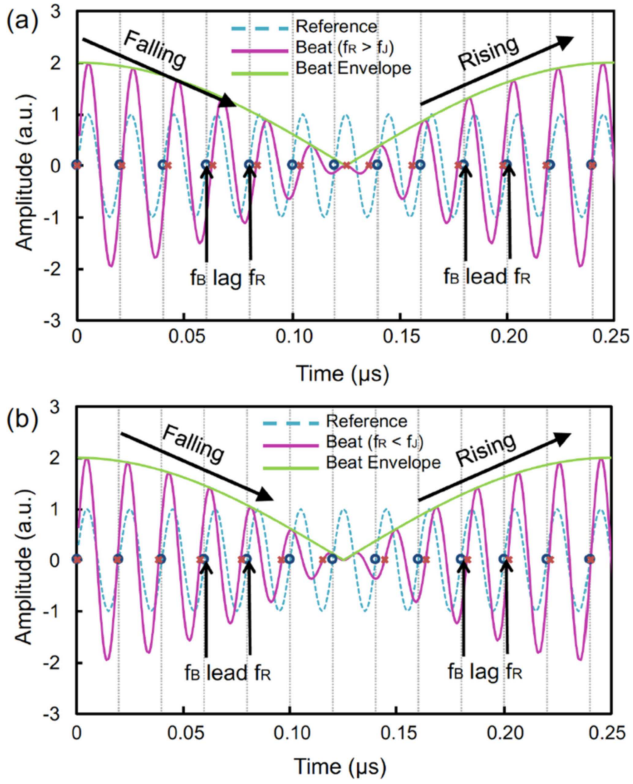

Fig. 9. Principle of the jamming avoidance response (JAR) in Eigenmannia. (a) When $f_R > f_J$, phase of beat signal is lagging the phase of the reference signal at the falling edge of the envelope, while it is leading at the rising edge. (b) When $f_R < f_J$, the phase of beat signal is leading the phase of the reference signal during the falling portion of the envelope, while it is lagging during the rising portion.

signal can be identified by comparing the positive zero crossing point of each signal. The positive zero crossing points of the reference signal are marked by the blue hollow circles, while the positive zero crossing points of the beat signal are marked by the red crosses. It is observed that the phase of the beat signal is lagging that of the reference signal during the beat signal's falling envelope; while it is leading the phase of the reference signal during the beat signal's rising envelope. However, as shown in Fig. 9(b), when the jamming signal f_J is at a higher frequency than the Eigenmannia's own signal f_R, the phase of the beat signal is leading that of the reference signal during the beat signal's falling envelope; while it is lagging the phase of the reference signal during the beat signal's rising envelope. Therefore, by extracting the amplitude change information in the beat signal as well as the phase relationship between the reference signal and beat signal, the JAR algorithm is capable of telling the Eigenmannia whether or not it should tune its emitting frequency to a higher or lower frequency to avoid potential jamming.

B. Optical Implementation of JAR for RF Systems

Due to the spectral scarcity and dramatic increasing demand of mobile RF devices/systems, inadvertent jamming is unavoidable. Inadvertent jamming is one type of jamming that comes from a friendly source, i.e. a nearby mobile radar, and is usually

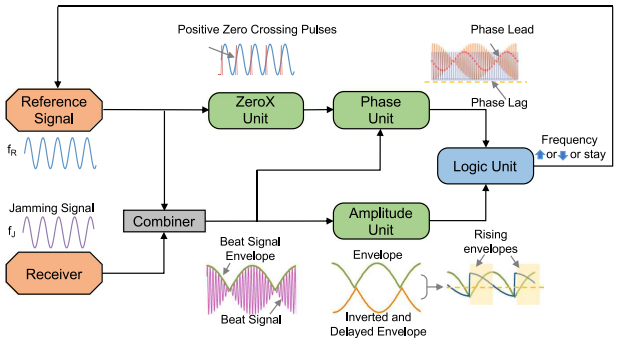

Fig. 10. Illustration of the JAR design and the four functional units – ZeroX unit, Phase unit, Amplitude unit, and Logic unit in JAR.

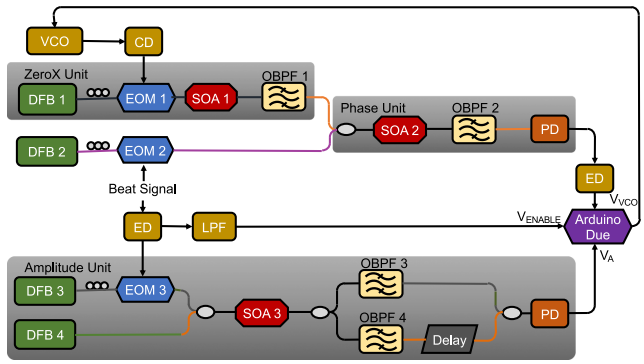

Fig. 11. Experimental setup of the photonic JAR that consists of the four functional units – ZeroX unit, Phase unit, Amplitude unit, and Logic unit.

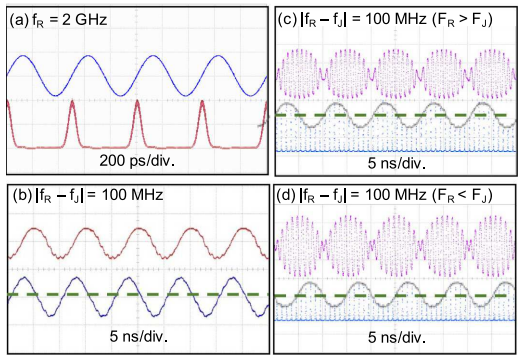

Fig. 12. Experimental results of the photonic-based JAR. Top curve: input; bottom curve: output. (a) ZeroX unit – positive zero crossing points of the reference signal (top blue) are identified and represented by the bottom red pulses. (c)–(d) Phase unit – the output amplitudes (bottom blue) are high for phase lag and are low for phase lead. (b) Amplitude unit – rising and falling in beat signal envelope amplitude (top red) are distinguished, a high output represents rising in amplitude and a low output represents falling in amplitude (bottom blue).

aimless and unforeseen. However, inadvertent jamming is as harmful as intentional jamming [52], [53] if jamming is not properly mitigated. Conventionally, inadvertent jamming could be avoided by careful spectral assignment, however, due to the spectral scarcity, mobility of RF systems, and the closely packed applications in the RF spectrum, it is becoming unrealistic to avoid inadvertent jamming through spectral assignment. Therefore, there is a critical need to identify an effective solution to tackle inadvertent jamming, which convention solution for intentional jamming will not work on inadvertent jamming. By examining the jamming issue in Eigenmannia, it has shown much similarity as in inadvertent jamming – meaning that the JAR in Eigenmannia could be a promising solution to inadvertent jamming in our wireless system. The biological JAR is working in the hundreds of Hz frequency range, using photonics to mimic JAR will able to bring the operation frequency to hundreds of MHz to tens of GHz range.

The JAR in Eigenmannia mainly consists of four functional blocks, as shown in Fig. 10 [41]–[44], they are (1) Zero-crossing point detection unit (ZeroX unit), (2) Phase detection unit (Phase Unit), (3) Amplitude unit, and (4) Logic unit. The ZeroX unit identifies the positive zero crossing points in the reference signal. Then, the Phase unit compares the phase relationship between the reference signal and the beat signal at the identified positive zero crossing points, and determine if the phase of the beat signal is leading or lagging that of the reference signal. Next, the Amplitude unit takes the envelope of the beat signal and identifies if the beat signal envelope is rising or falling in amplitude. Finally, the Logic unit takes the phase and amplitude information from the outputs of the Phase unit and Amplitude unit and determines if the emitting frequency of the Eigenmannia should be remained, increased, or decreased. In Eigenmannia, the JAR is only enabled if the frequency difference between the Eigenmannia emitting frequency and the jamming frequency are within the jamming range, otherwise, the emitting frequency is maintained.

The photonic implementation of JAR is shown in Fig. 11. The major devices to achieve the JAR is semiconductor optical amplifier (SOA), and various photonic phenomena in SOA is being utilized. SOA has been used as a spiking processing device for mimicking neuron behavior with picosecond response time, and here, SOA's application in implementing JAR is discussed.

First, the reference signal from a voltage control oscillator (VCO) and the beat signal are modulated onto three optical carriers generated from distributed laser diodes (DFB 1–3) at different wavelength. As the reference signal (Blue waveform in Fig. 12(a)) enters the SOA1, it induces self-phase modulation and causes spectral broadening in the optical spectrum. An optical filter is used to select the portion of the optical spectrum that corresponding to the positive zero crossing point at the reference signal, resulting in pulses at each positive zero crossing points, as shown by the red waveform in Fig. 12(a). Then, the zero-crossing point pulses together with the beat signal (pink curves in Fig. 12(c) and (d)) are launched to SOA2.

The beat signal is the strong pump that could induce cross-gain modulation in the SOA, while the zero crossing point pulses are the weak probe that experience cross-gain modulation. If the phase of the beat signal is leading, the beat signal depletes the carriers in the SOA, such that the zero crossing pulses experience very weak or no gain – a weak output is resulted. However, if the phase of the beat signal is lagging, the zero crossing pulses leaves the SOA before cross gain modulation is induced by the beat signal, therefore, the zero crossing pulses will have strong output power. In short, a "0" is resulted if the phase of the beat

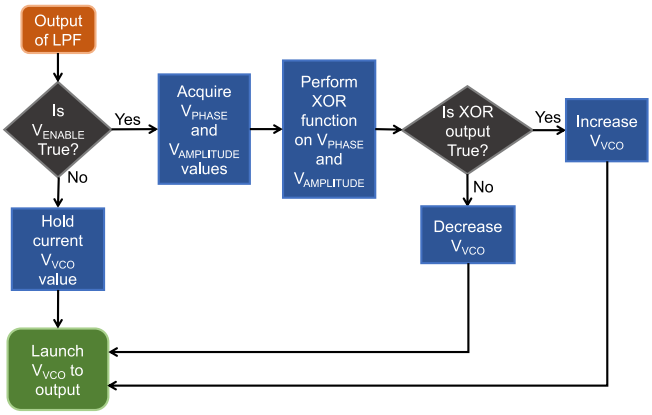

Fig. 13. The logic flow chat of the logic unit. V_{PHASE}: Phase information from the Phase unit; $V_{AMPLITUDE}$: Amplitude information from the Amplitude unit; V_{VCO}: Current setting at the V_{CO}; V_{enable}: Output from the low pass filter determining if the jamming frequency is within the jamming range.

signal is leading, while a "1" is resulted if the phase of the beat signal is lagging, as shown in Fig. 12(c) and (d). The amplitude unit takes the beat signal envelope and launches it to SOA3 together with a continuous light wave from DFB 4. With the beat signal envelope as the pump light to deplete the carrier in the SOA, an inverted copy of it is resulted at the DFB 4 output. Relative delay is introduced between the inverted copy and non-inverted copy of the beat signal envelope, such that a weak output is resulted during the falling beat signal envelope while a strong output is resulted during the rising beat signal envelope, as shown in Fig. 12(b).

In the photonic JAR, an electrical low pass filter (LPF) is used to determine whether the JAR should be enabled. If the frequency difference between the reference signal and jamming signal is smaller than the LPF frequency, i.e. within the jamming range, then JAR is enabled, and the reference frequency will either move higher or lower according to the result from the JAR; otherwise, the JAR is disabled, and the reference frequency is maintained.

Fig. 13 shows the operation principle of the logic circuit. Since the amplitude and phase information are now down to a low frequency range, determined by the frequency difference between f_R and f_J. i.e., same as the beat signal envelope (i.e., around 200 MHz), an Arduino Due is used instead of photonic circuit to implement the Logic unit.

Once the JAR is enabled to shift the reference signal frequency step by step, the Logic unit also responsible to determine when to stop the shifting of frequency. The shifting of reference signal frequency should stop once the jamming frequency is out of the jamming frequency range of the reference signal from the first Eigenmannia. Fig. 14 shows the spectral waterfall measurement of the photonic JAR in action. The jamming signal is approaching the Eigenmannia from either lower or higher frequency and the JAR helps the Eigenmannia to keep its emitting frequency to be out of the jamming frequency range. The photonic JAR will also work when the reference signal is modulated digitally or analogy. The photonic JAR supports frequency from hundreds of MHz to tens of GHz, with jamming sensitivity defined by the

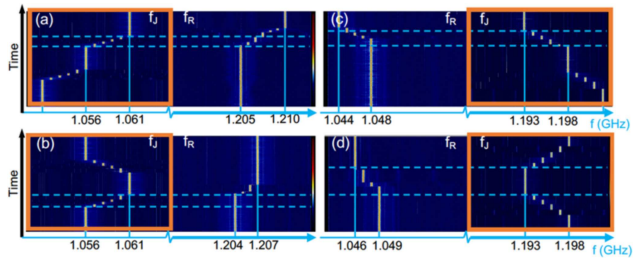

Fig. 14. Spectral waterfall measurement of the photonic JAR in action with sinusoidal reference signal f_R and jamming signals $f_J = 150$ MHz. (a) f_J is approaching f_R from the low frequency side and triggers the JAR, (b) f_J is approaching f_R from the low frequency side and triggers the JAR, and then is moved away, (c) f_J is approaching f_R from the high frequency side and triggers the JAR, (d) f_J is approaching f_R from the high frequency side and triggers the JAR and then is moved away.

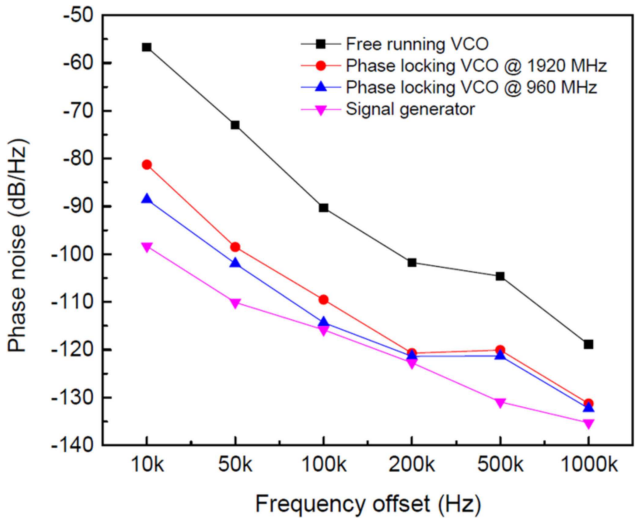

Fig. 15. Phase noise improvement of a VCO using the JAR based phase lock loop.

bandwidth of the RF low-pass filter. The major advantage of JAR for avoiding inadvertent jamming is its effectiveness towards an unknown jamming frequency with no prior knowledge needed, its wide operation frequency range, and its analog processing. However, intensive research is still needed to modify the JAR for scenario with multiple jammers.

Besides using the photonic JAR for inadvertent jamming, another application is to use the ZeroX unit and Phase unit for detecting the phase difference in a phase lock loop [39]. Experimental demonstration shows that the photonic JAR based microwave phase lock loop has significantly suppressed the phase noise of a voltage-controlled oscillator (VCO) by 25 dB, as shown in Fig. 15.

IV. Summary and Discussion

Interdisciplinary applications of neural science have been a very interesting field to explore and there are a lot of useful neural algorithms that could be a good candidate for solving long lasting challenges in human technologies. Neural algorithm has undergone hundreds of million years of evolution and are optimized to effectively perform designated tasks. In

just a short ten years, intensive research has been focusing on the photonic demonstration of spiking neuron, synapse, neural network, and various small scale neural algorithms, that could essentially allow the effective but slow neural algorithm to operate at a fast time scale of picoseconds [47]. Photonic implementation of small scale functional neural algorithms is not trivial. First, most functional neural algorithms are hard to dissect and understand even by neuroscientist. Very often, neural behaviors are being observed without a clear explanation of how it works. Therefore, implementing functional neural algorithm requires the identification of well-studied neural algorithm, evaluation of the potential benefit to human society, translating the neural algorithm to an engineering problem, and implementing the engineering-translated neural algorithm using optical phenomena.

This paper discusses the idea of marrying photonics with neural science and presents a number of neural-inspired photonic circuits that mimic various neural functional algorithms using optical devices and optical phenomena. Neural algorithms have find its value in solving challenges in various RF signal processing applications, by providing efficient, accurate, and task-specific capabilities. The photonic implementation of neural algorithms that are introduced in this paper including angle-of-arrival measurement, 3D indoor localization, phase-lock-loop, and inadvertent jamming avoidance in wireless RF systems. There are still lots of hidden treasure in the nature that are waiting to be explored and could be an effective solution to the challenges we are facing in the modern society.

ACKNOWLEDGMENT

M. P. Fok would like to thank Dr. David Rosenbluth from Lockheed Martin and Prof. Paul Prucnal from Princeton University for the fruitful discussion on the project.

REFERENCES

[1] D. Rosenbluth, K. Kravtsov, M. P. Fok, and P. R. Prucnal, "A high performance photonic pulse processing device," *Opt. Express*, vol. 17, no. 25, pp. 22767–22772, 2009.

[2] M. P. Fok, D. Rosenbluth, K. Kravtsov, and P. R. Prucnal, "Lightwave neuromorphic signal processing," *IEEE Signal Process. Mag.*, vol. 27, no. 6, pp. 158–160, Nov. 2010.

[3] K. Kravtsov, M. P. Fok, D. Rosenbluth, and P. R. Prucnal, "Ultrafast all-optical implementation of a leaky integrate-and-fire neuron," *Opt. Express*, vol. 19, no. 3, pp. 2133–2147, 2011.

[4] M. P. Fok, Y. Tian, D. Rosenbluth, and P. R. Prucnal, "Asynchronous spiking photonic neuron for lightwave neuromorphic signal processing," *Opt. Lett.*, vol. 37, no. 16, pp. 3309–3311, 2012.

[5] A. Hurtado, K. Schires, I. D. Henning, and M. J. Adams, "Investigation of vertical cavity surface emitting laser dynamics for neuromorphic photonic systems," *Appl. Phys. Lett.*, vol. 100, no. 10, 2012, Art. no. 103703.

[6] M. A. Nahmias, B. J. Shastri, A. N. Tait, and P. R. Prucnal, "A leaky integrate-and-fire laser neuron for ultrafast congnitive computing," *IEEE J. Sel. Top. Quantum Electron.*, vol. 19, no. 5, pp. 1–12, Sep. /Oct. 2013.

[7] F. Selmi, F. R. Braive, G. Beaudoin, I. Sagnes, R. Kuszelewicz, and S. Barbay, "Temporal summation in a neuromimetic micropillar laser," *Opt. Lett.*, vol. 40, no. 23, pp. 5690–5693, 2015.

[8] T. Deng, J. Robertson, and A. Hurtado, "Controlled propagation of spiking dynamics in vertical-cavity surface-emitting lasers: Towards neuromorphic photonic networks," *IEEE J. Sel. Top. Quantum Electron.*, vol. 23, no. 6, pp. 1–8, Nov. /Dec. 2017.

[9] A. N. Tait *et al.*, "A silicon photonic modulator neuron," *Appl. Phys.*, 2018, *arXiv:1812.11898.*

[10] B. J. Shastri, M. A. Nahmias, A. N. Tian, B. Wu, and P. R. Prucnal, "Graphene excitable laser for photonic spike processing," in *Proc. IEEE Photon. Conf.*, 2013, pp. 1–2.

[11] V. Vaerenbergh *et al.*, "Cascadable excitability in microrings," *Opt. Express*, vol. 20, no. 18, pp. 20292–20308, 2012.

[12] K. Alexander, T. Van Vaerenbergh, M. Fiers, P. Mechet, J. Dambre, and P. Bienstman, "Excitability in optically injected microdisk lasers with phase controlled excitatory and inhibitory response," *Opt. Express*, vol. 21, no. 22, pp. 26182–26191, 2013.

[13] B. J. Shastri, M. A. Nahmias, A. N. Tait, and P. R. Prucnal, "Simulation of a graphene excitable laser for spike processing," *Opt. Quantum Electron.*, vol. 46, no. 10, pp. 1353–1358, 2014.

[14] B. J. Shastri, M. A. Nahmias, A. N. Tait, B. Wu, and P. R. Prucnal, "SIMPEL: Circuit model for photonic spike processing laser neurons," *Opt. Express*, vol. 23, no. 6, pp. 8029–8044, 2015.

[15] M. A. Nahmias, A. N. Tait, B. J. Shastri, T. F. de Lima, and P. R. Prucnal, "Excitable laser processing network node in hybrid silicon: Analysis and simulation," *Opt. Express*, vol. 23, no. 20, pp. 26800–26813, 2015.

[16] B. J. Shastri, M. A. Nahmias, A. N. Tait, A. W. Rodriguez, B. Wu, and P. R. Prucnal, "Spike processing with a graphene excitable laser," *Scientific Rep.*, vol. 6, 2016, Art. no. 19126.

[17] I. Chakraborty, G. Saha, A. Sengupta, and K. Roy, "Toward fast neural computing using all-photonic phase change spiking neurons," *Scientific Rep.*, vol. 8, no. 1, pp. 1–9, 2018.

[18] P. Y. Ma, B. J. Shastri, A. N. Tait, M. A. Nahmias, T. F. de Lima, and P. R. Prucnal, "Simultaneous excitory and inhibitory dynamics in a graphene excitable laser," *Opt. Lett.*, vol. 43, no. 15, pp. 3802–3805, 2018.

[19] Z. Cheng, C. Ríos, W. H. Pernice, C. D. Wright, and H. Bhaskaran, "On-chip photonic synapse," *Sci. Adv.*, vol. 3, no. 9, 2017, Art. no. e1700160.

[20] B. Romeira, R. Avó, J. M. Figueiredo, S. Barland, and J. Javaloyes, "Regenerative memory in time-delayed neuromorphic photonic resonators," *Scientific Rep.*, vol. 6, 2016, Art. no. 19510.

[21] X. Zhuge, J. Wang, and F. Zhuge, "Photonic synapses for ultrahigh-speed neuromorphic computing," *Phy. Status Solidi (RRL)–Rapid Res. Lett.*, vol. 13, no. 9, 2019, Art. no. 1900082.

[22] B. Gholipour, P. Bastock, C. Craig, K. Khan, D. Hewak, and C. Soci, "Amorphous metal-sulphide microfibers enable photonic synapses for brain-like computing," *Adv. Opt. Mater.*, vol. 3, no. 5, pp. 635–641, 2015.

[23] Z. Song, S. Xiang, Z. Ren, G. Han, and Y. Hao, "Spike sequence learning in a photonic spiking neural network consisting of VCSELs-SA with supervised training," in *IEEE J. Sel. Top. Quantum Electron.*, vol. 26, no. 5, pp. 1–9, Sep./Oct. 2020, Art no. 1700209.

[24] J. Feldmann, N. Youngblood, C. David Wright, H. Bhaskaran, and W. H. P. Pernice, "All-optical spiking neurosynaptic networks with self-learning capabilities," *Nature*, vol. 569, no. 7755, pp. 208–214, 2019.

[25] A. N. Tait, M. A. Nahmias, B. J. Shastri, and P. R. Prucnal, "Broadcast and weight: An integrated network for scalable photonic spike processing," *J. Lightw. Technol.*, vol. 32, no. 21, pp. 3427–3439, Nov. 2014.

[26] M. A. Nahmias, A. N. Tait, B. J. Shastri, T. F. de Lima, and P. R. Prucnal, "Excitable laser processing network node in hybride silicon: Analysis and simulation," *Opt. Express*, vol. 23, no. 20, pp. 26800–26813, 2015.

[27] J. M. Shainline, S. M. Buckley, P. R. Mirin, and S. W. Nam, "Superconducting optoelectronic circuits for neuromorphic computing," *Phys. Rev. Appl.*, vol. 7, no. 3, 2017, Art. no. 034013.

[28] A. N. Tait *et al.*, "Neuromorphic photonic networks using silicon photonic weight banks," *Scientific Reports*, vol. 7, no. 1, 2017, Art. no. 7430.

[29] M. P. Fok *et al.*, "Signal feature recognition based on lightwave neuromorphic signal processing," *Opt. Lett.*, vol. 36, no. 1, pp. 19–21, 2011.

[30] R. Toole and M. P. Fok. "Photonic implementation of a neuronal learning algorithm based on spike timing dependent plasticity," in *Proc. Opt. Fiber Commun. Conf.*, 2015, Paper W1K-6.

[31] R. Toole and M. P. Fok, "Photonic implementation of a neuronal algorithm applicable towards angle of arrival detection and localization," *Opt. Express*, vol. 23, no. 12, pp. 16133–16141, 2015.

[32] S. Xiang, Y. Zhang, J. Gong, X. Guo, L. Lin, and Y. Hao, "STDP-based unsupervised spike pattern learning in a photonic spiking neural network with VCSELs and VCSOAs," *IEEE J. Sel. Top. Quantum Electron.*, vol. 25, no. 6, pp. 1–9, Nov. /Dec. 2019.

[33] C. Mesaritakis, M. Skontranis, G. Sarantoglou, and A. Bogris, "Micro-ring-resonator based passive photonic spike-time-dependent-plasticity scheme for unsupervised learning in optical neural networks," in *Proc. Opt. Fiber Commun. Conf. OSA Tech. Digest Opt. Soc. Amer.*, 2020, pp. 1–3.

[34] M. P. Fok, Y. Tian, D. Rosenbluth, and P. R. Prucnal, "Pulse lead/lag timing detection for adaptive feedback and control based on optical spike-timing-dependent plasticity," *Opt. Lett.*, vol. 38, no. 4, pp. 419–421, 2013.

[35] R. Toole *et al.* "Photonic implementation of spike timing dependent plasticity and learning algorithms of biological neural systems," *J. Lightw. Technol.*, vol. 34, no. 2, pp. 470–476, Jan. 2016.
[36] T. F. de Lima *et al.*, "Machine learning with neuromorphic photonics," *J. Lightw. Technol.*, vol. 37, no. 5, pp. 1515–1534, Mar. 2019.
[37] Y. Shen *et al.*, "Deep learning with coherent nanophotonic circuits," *Nature Photon.*, vol. 11, no. 7, 2017, Art. no. 441.
[38] T. F. de Lima, A. Tait, M.A. Nahmias, B. J. Shastri, and P. R. Prucnal, "Scable wideband principal component analysis via microwave photonics," *IEEE Photon. J.*, vol. 8, no. 2, pp. 1–9, Apr. 2016.
[39] J. Bueno, S. Maktoobi, L. Froehly, I. Fischer, M. Jacquot, L. Larger, and D. Brunner, "Reinforcement learning in a large-scale photonic recurrent neural network," *Optica*, vol. 5, no. 6, pp. 756–760, 2018.
[40] A. N. Tait, J. Chang, B. J. Shastri, M. A. Nahmias, and P. R. Prucnal, "Demonstratino of WDM weighted addition for principal component analysis," *Opt. Express*, vol. 23, no. 10, pp. 12758–12765, 2015.
[41] R. Toole and M. P. Fok, "A photonic RF jamming avoidance response system bio-inspired by Eigenmannia," in *Proc. Opt. Fiber Commun. Conf. Expo.*, 2016, pp. 1–3.
[42] M. P. Fok and R. Toole, "Photonic Approach for RF jamming Avoidance Response System Inspired by the fish – Eigenmannia," *IEEE Photon. Soc. Newsletter – Res. Highlights*, vol. 29, no. 6, pp. 4–9, 2015.
[43] M. P. Fok and R. Toole, "Photonic implementation of jamming avoidance response (JAR) in Eigenmannia," U.S. Utility Patent, S/N: 62/246, 903.
[44] R. Lin, J. Ge, T. P. T. Do, L. A. Perea, R. Toole, and M. P. Fok, "Biomimetic photonics – Jamming avoidance system in Eigenmannia," *Opt. Express*, vol. 26, no. 10, pp. 13349–13360, 2018.
[45] R. Lin, L. Perea, T. P. Do, J. Ge, L. Xu, and M. P. Fok, "Bio-inspired optical microwave phase lock loop based on nonlinear effects in semiconductor optical amplifier," *Opt. Fiber Commun. Conf. Expo.*, pp. 1–3, 2017.
[46] S. Song, K. D. Miller, and L. F. Abbott, "Competitive Hebbian learning through spike-timing-dependent synaptic plasticity," in *Nature Neurosci.*, vol. 3, pp. 919–926, 2000.
[47] T. H. Bullock, R. H. Hamstra, and H. Scheich, "The jamming avoidance response of high frequency electric fish," *How do Brains Work?*, Birkhäuser Boston: Springer, 1993, pp. 509–534.
[48] H. Scheich, "Neural basis of communication in the high frequency electric fish, Eigenmannia virescens (jamming avoidance response)," *J. Comparative Physiol.*, vol. 113, no. 2, pp. 181–206, 1977.
[49] W. Heiligenberg and G. Rose, "Phase and amplitude computations in the midbrain of an electric fish: Intracellular studies of neurons participating in the jamming avoidance response of Eigenmannia," *J. Neurosci.*, vol. 5, no. 2, pp. 515–531, 1985.
[50] W. Metzner, "The jamming avoidance response in Eigenmannia is controlled by two separate motor pathways," *J. Neurosci.*, vol. 13, no. 5, pp. 1862–1878, 1993.
[51] S. A. Stamper, M. S. Madhav, N. J. Cowan, and E. S. Fortune, "Beyond the jamming avoidance response: Weakly electric fish respond to the envelope of social electrosensory signals," *J. Experimnetal Biol.*, vol. 215, no. 23, pp. 4196–4207, 2012.
[52] M. Wilhelm, I. Martinovic, J. B. Schmitt, and V. Lenders, "Short paper: Reactive jamming in wireless networks: How realistic is the threat?," in *Proc. Fourth ACM Conf. Wireless Netw. Secur.*, 2011, pp. 47–52.
[53] R. A. Poisel, "Modern communications jamming principles and techniques," *Artech House*, Artech House Inc., 2011.
[54] M. P. Fok, "Neuromorphic photonics for RF signal processing," in *Proc. Int. Top. Meet. Microw. Photon.*, Ottawa, Canada, Oct. 7-10, 2019, pp. 1–5.

Mable P. Fok (Member, IEEE) received the B.Eng., M.Phil., and Ph.D. degrees in electronic engineering from the Chinese University of Hong Kong (CUHK), Hong Kong, in 2002, 2004, and 2007, respectively. She was a Visiting Researcher at the University of California, Los Angeles (UCLA), CA, USA, and the University of California, Santa Barbara (UCSB), CA, USA, during 2005 and 2006, respectively, where she was engaged in the research on supercontinuum generation in nonlinear fibers with the former and all-optical processing of advanced modulation format signals with the later After graduation, Dr. Fok joined the Department of Electrical Engineering at Princeton University, Princeton, NJ, USA, as an Associate Research Scholar in 2007, where she was focusing on hybrid analog/digital processing of optical signals based on neuromorphic algorithm and developing new techniques to enhance physical layer information security in optical communications network.

She is currently an Associate Professor and a Distinguished Faculty Fellow with the College of Engineering at the University of Georgia, Athens, GA, USA. She has published over 200 journal and conference papers. Her recent research interest is on photonic implementation of neuromorphic algorithm, developing new photonic techniques for dynamic and flexible RF communication systems, and designing bio-inspired soft robotics.

Dr. Fok is the recipient of the 2017 NSF CAREER award, 2019 Creative Research Medal, 2016 CURO Research Mentoring Award, 2015 College of Engineering Excellence in Research Faculty Award, 2014 Ralph E. Powe Junior Faculty Enhancement Award from ORAU, and 2010 IEEE Photonics Society Graduate Student Fellowship.